

## Experiment Report Form

**The double page inside this form is to be filled in by all users or groups of users who have had access to beam time for measurements at the ESRF.**

Once completed, the report should be submitted electronically to the User Office via the User Portal:

<https://www.esrf.fr/misapps/SMISWebClient/protected/welcome.do>

### ***Reports supporting requests for additional beam time***

Reports can be submitted independently of new proposals – it is necessary simply to indicate the number of the report(s) supporting a new proposal on the proposal form.

The Review Committees reserve the right to reject new proposals from groups who have not reported on the use of beam time allocated previously.

### ***Reports on experiments relating to long term projects***

Proposers awarded beam time for a long term project are required to submit an interim report at the end of each year, irrespective of the number of shifts of beam time they have used.

### ***Published papers***

All users must give proper credit to ESRF staff members and proper mention to ESRF facilities which were essential for the results described in any ensuing publication. Further, they are obliged to send to the Joint ESRF/ ILL library the complete reference and the abstract of all papers appearing in print, and resulting from the use of the ESRF.

Should you wish to make more general comments on the experiment, please note them on the User Evaluation Form, and send both the Report and the Evaluation Form to the User Office.

### **Deadlines for submission of Experimental Reports**

- 1st March for experiments carried out up until June of the previous year;
- 1st September for experiments carried out up until January of the same year.

### **Instructions for preparing your Report**

- fill in a separate form for each project or series of measurements.
- type your report, in English.
- include the reference number of the proposal to which the report refers.
- make sure that the text, tables and figures fit into the space available.
- if your work is published or is in press, you may prefer to paste in the abstract, and add full reference details. If the abstract is in a language other than English, please include an English translation.



	<b>Experiment title:</b> In situ atomic structure and catalytic properties relationship for the palladium catalyst under industrially relevant conditions	<b>Experiment number:</b> CH- 4871
<b>Beamline:</b> BM26A	<b>Date of experiment:</b> from: 01.12.2016 to: 08.12.2016	<b>Date of report:</b> 10.03.2017
<b>Shifts:</b> 21	<b>Local contact(s):</b> Alessandro Longo ( email: alessandro.longo@esrf.fr )	<i>Received at ESRF:</i>
<b>Names and affiliations of applicants</b> (* indicates experimentalists): Aram Bugaev* <sup>1,2</sup> , Alexander Guda* <sup>1</sup> , Andrea Lazzarini <sup>2</sup> , Kirill Lomachenko <sup>1,2</sup> , Elena Groppo <sup>2</sup> , Alexander Soldatov <sup>1</sup> , Jeroen van Bokhoven <sup>3,4</sup> , Carlo Lamberti* <sup>1,2</sup> + Ilia Pankin* <sup>1</sup> , Victor Shapovalov* <sup>1</sup> , and Yuri Rusalev* <sup>1</sup> <sup>1</sup> Southern Federal University, Zorge street 5, 344090 Rostov-on-Don, Russia <sup>2</sup> Department of Chemistry, University of Turin, Via P. Giuria 7, 10125 Turin, Italy <sup>3</sup> Institute for Chemical and Bioengineering, ETH Zurich, HCI E127 8093 Zurich <sup>4</sup> Laboratory for Catalysis and Sustainable Chemistry (LSK), Swiss Light Source, Paul		

## Report:

Palladium nanoparticles are extensively used in catalysis, in particular, for the hydrogenation of unsaturated hydrocarbons. Under reaction condition palladium catalyst may undergo a transition to its hydride or carbide phases, which change dramatically the catalytic properties of the material. The aim of this experiment was to investigate the relationship between the structure and catalytic properties of the palladium nanoparticles supported on carbon in a model reaction of ethylene to ethane hydrogenation by means of in situ X-ray absorption spectroscopy. In addition, the five additional shifts which were allocated in the end of the experiment were focused on the study of the catalytic activity of ruthenium nanoparticles.

### **I. In situ atomic structure and catalytic properties relationship for the palladium nanoparticles during ethylene to ethane hydrogenation**

The experiment was performed at BM26B beamline. Palladium nanoparticles were loaded inside the in situ cell shown in Figure 1.1, between two graphite windows allowing us to collect X-ray absorption spectra in transmission mode. The data collection was performed at Pd K-edge in the range from 24.15 till 25.15 keV. The input of the cell was connected to a remotely controlled gas rig of the BM26B, allowing to adjust the gas composition and flow through the cell. The two main reacting gasses were hydrogen and ethylene, while helium was used as a carrier inert gas. The output of the cell was connected to the mass spectrometer to control the resulting gas mixture after the catalytic reaction.

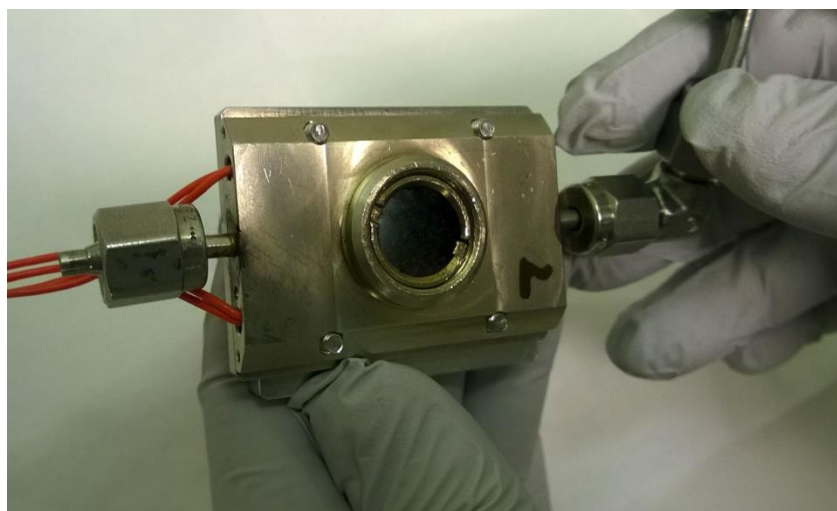


Figure 1.1. In situ cell for XAS measurements.

Being exposed to air, palladium nanoparticles are easily oxidized. Therefore, each time when the new sample was loaded, we were making pretreatment in hydrogen at 120 °C which reduce nanoparticles, removing surface oxygen.

After the reduction, the sample was cooled down to 80 °C, the temperature at which all the catalytic tests were performed. The starting flow of 15 ml/min of hydrogen and 35 ml/min of helium provided the  $\beta$ -hydride phase of the palladium nanoparticles with interatomic  $R_{\text{Pd-Pd}}$  distance equal to  $2.81 \pm 0.01 \text{ \AA}$  as determined by single shell Fourier-analysis of EXAFS spectra. During the following steps the ethylene flow was added stepwise from 0 to 10 ml/min. At each step EXAFS spectrum was acquired. Mass spectrum was recorded continuously.

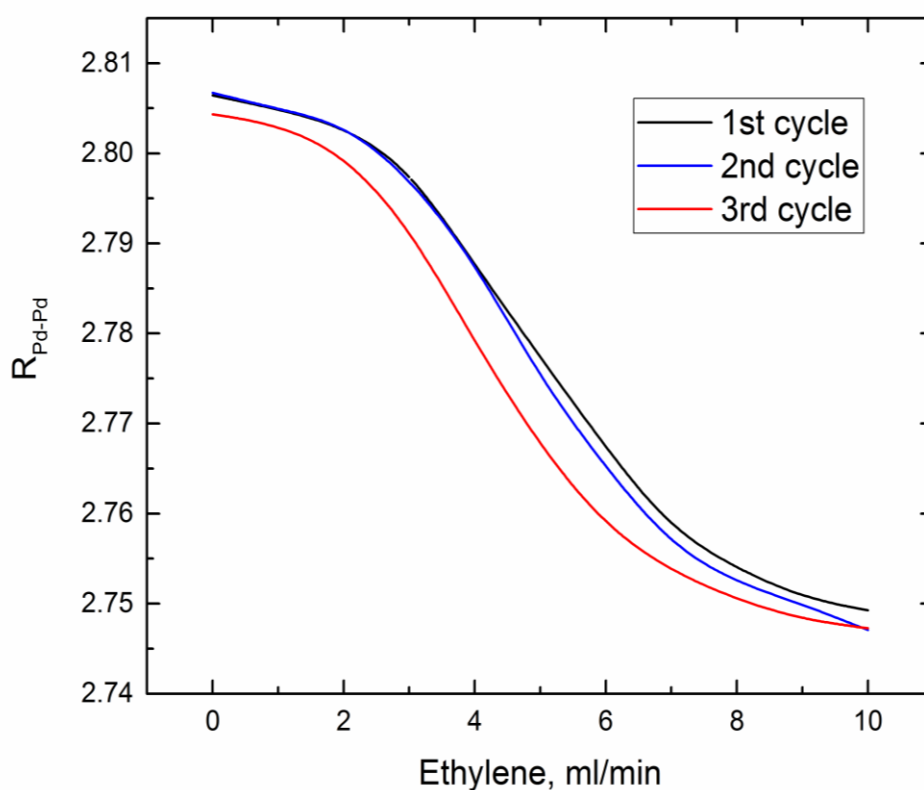


Figure 1.2. Results of the EXAFS analysis during three cycles of the catalytic reaction.

The results of the single-shell Fourier analysis are presented in Figure 1.2. It can be seen that starting from the ethylene flow of 3 ml/min we observed decreasing of  $R_{\text{Pd-Pd}}$  distance down to  $2.75 \pm 0.01 \text{ \AA}$ . This decrease is caused by the fact that a catalytic reaction of ethylene to ethane hydrogenation leads to a consumption of hydrogen lowering the partial hydrogen pressure and leading to the decomposition of the  $\beta$ -phase. The next cycle shows that the  $\beta$ -phase is formed back almost irreversibly, however its decomposition started at slightly lower ethylene flow. The next cycle demonstrate even bigger deviation of the  $R_{\text{Pd-Pd}}$  distance behavior. This indicates that a fraction of the palladium carbide phase is irreversibly formed, which changes the thermodynamic of pure Pd-H system. After this cycle the sample was changed to a fresh one. The corresponding MS data are shown in the Figure 1.3. Three first cycles which have been discussed in the previous paragraph are represented on abscissa axis from #Cycle = 1000 to #Cycle = 22000. The #Cycle from 40000 to 48000 correspond to the same catalytic procedure applied to a fresh loaded sample. Term #Cycle means the number of mass spectrometer internal cycle which takes iteratively a response of the set of fragments of interest. As the absolute values of the mass spectrometer cannot be used directly for quantitative analysis due to the drift of MS, we present the responses of different fragments divided one by another. For example, the value 30/26 (figure 1.3, red) is close to 1 for pure ethane and is close to 0 for pure ethylene, which was tested in the independent experiment with the same mass spectrometer using pure gasses without a catalyst.

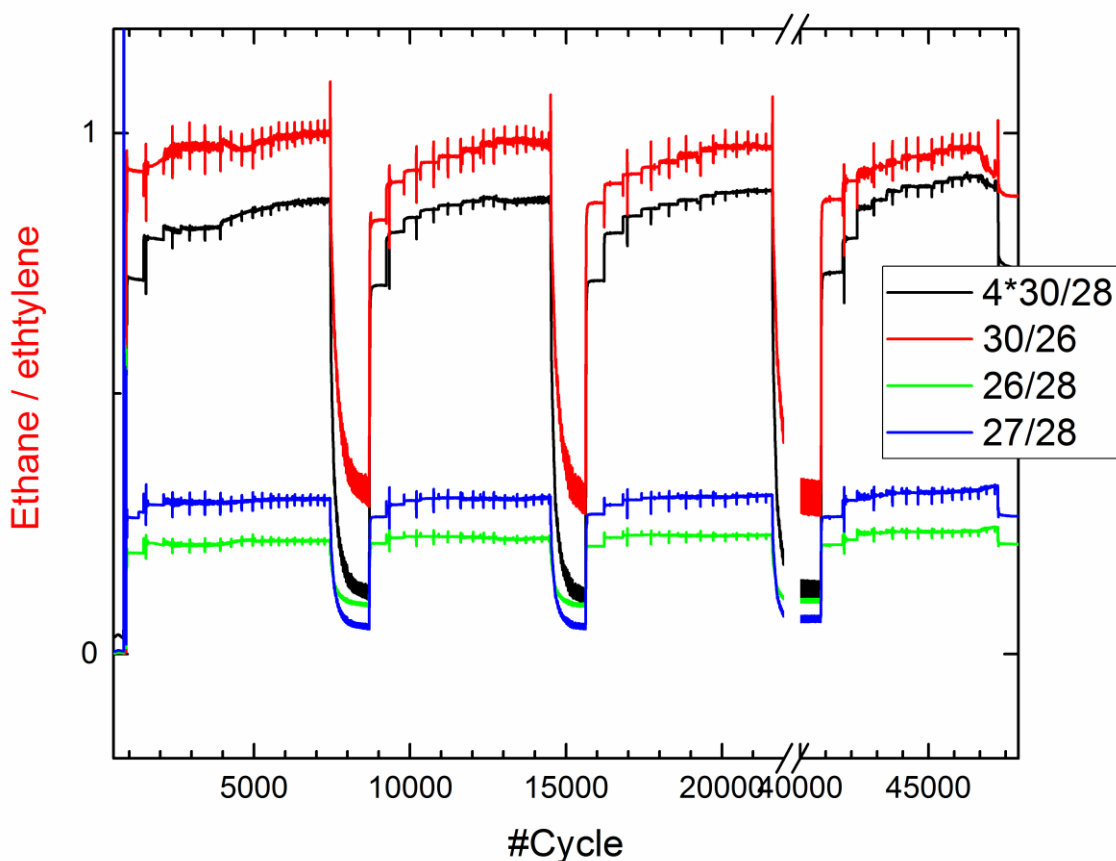


Figure 1.3. MS data. For quantitative treatment of data, we present not the initial mass spectrum but signals of the different fragment corresponding to ethylene and ethane divided one by another. #Cycle means the number of the internal cycle of mass spectrometer.

The most peculiar fact is that despite extremely high catalytic activity which is expected for the palladium nanoparticles for the reaction of ethylene hydrogenation, at the beginning of each cycle, when the ethylene flow is low, the conversion of ethylene is smaller than in the end of the cycle, where the ethylene flow is 10 times higher. As it is known that the ethylene hydrogenation is either zero or negative order reaction with respect to ethylene, this observation evidence the role of the catalyst. In particular, one preliminary conclusion is the following: the pre-hydrogenated catalyst is less performing than the catalyst which is already exposed to the catalytic mixture; the reason for such phenomena is the carbide phase which is formed in the palladium nanoparticles.

To confirm this fact the further analysis of XANES region of the spectra will be performed. This will include principle component analysis of all the spectra and direct calculation of XANES by FDMNES code. Also, part of the data have not been analyzed yet, which includes the similar catalytic cycle performed for the catalyst previously exposed to pure ethylene. This was done to test, how the pre-carbided catalyst would behave in comparison with pre-hydrogenated one.

In addition, based on the data collected during previous beamtimes, we have recently completed a manuscript entitled: “Core-shell structure of palladium hydride nanoparticles revealed by combined X-ray absorption spectroscopy and X-ray diffraction”, which is currently under consideration in the Journal of Physical Chemistry C. The abstract of the manuscript is given below:

We studied in situ 2.6 nm palladium nanoparticles supported on active carbon during the process of hydride phase formation. A core-shell structure was highlighted in the single-component particles on the basis of a different atomic structure and electronic configurations in the inner “core” and surface “shell” regions. The atomic structure of these particles was examined by combined X-ray powder diffraction (XRPD) which is sensitive mainly to a crystalline core region of the nanoparticles and extended X-ray absorption fine structure (EXAFS) which reflects the averaged structure of both core and more disordered shell. XRPD analysis confirms the existence of two well-separated  $\alpha$ - and  $\beta$ - hydride phases with characteristic flat plateau in the phase transition region of the pressure-distance isotherms. In contrast, interatomic distances obtained from EXAFS exhibit smoother behavior in the phase transition region, typical for nanostructured palladium. Such difference is explained by distinct properties of bulk “core” which has crystalline structure and sharp phase transition, and surface “shell” which is amorphous and absorbs hydrogen gradually without forming distinguishable  $\alpha$ - and  $\beta$ - phases. Combining EXAFS and XRPD we were able to extract the Pd-Pd first-shell distance in the amorphous shell of the nanoparticles, that is significantly shorter than in the bulk core. Additionally, we demonstrated the differences in the evolution of the Debye-Waller parameters obtained from EXAFS and XRPD along the hydride phase formation.

## II. In situ atomic structure and catalytic properties relationship for the ruthenium nanoparticles during their formation and catalytic reaction of ethanol oxidation

Formation of Ru nanoparticles was observed in situ. We started from the ruthenium chloride precursor which was heated in 20% O<sub>2</sub> in He leading to the formation RuO<sub>2</sub> nanoarticles. The following treatment in hydrogen reduces the nanoparticles to pure Ru ones. This process can be seen from the evolution of Ru-O and Ru-Ru first-shell contributions to EXAFS (Figure 2.1). Indeed, after oxidation, we are forming an oxide phase, with a first O shell around 2 Å and a higher Ru shell around 3.5 Å. The second Ru shell has only 2 neighbors and is much less apparent in the figure (small contribution around 3 Å).

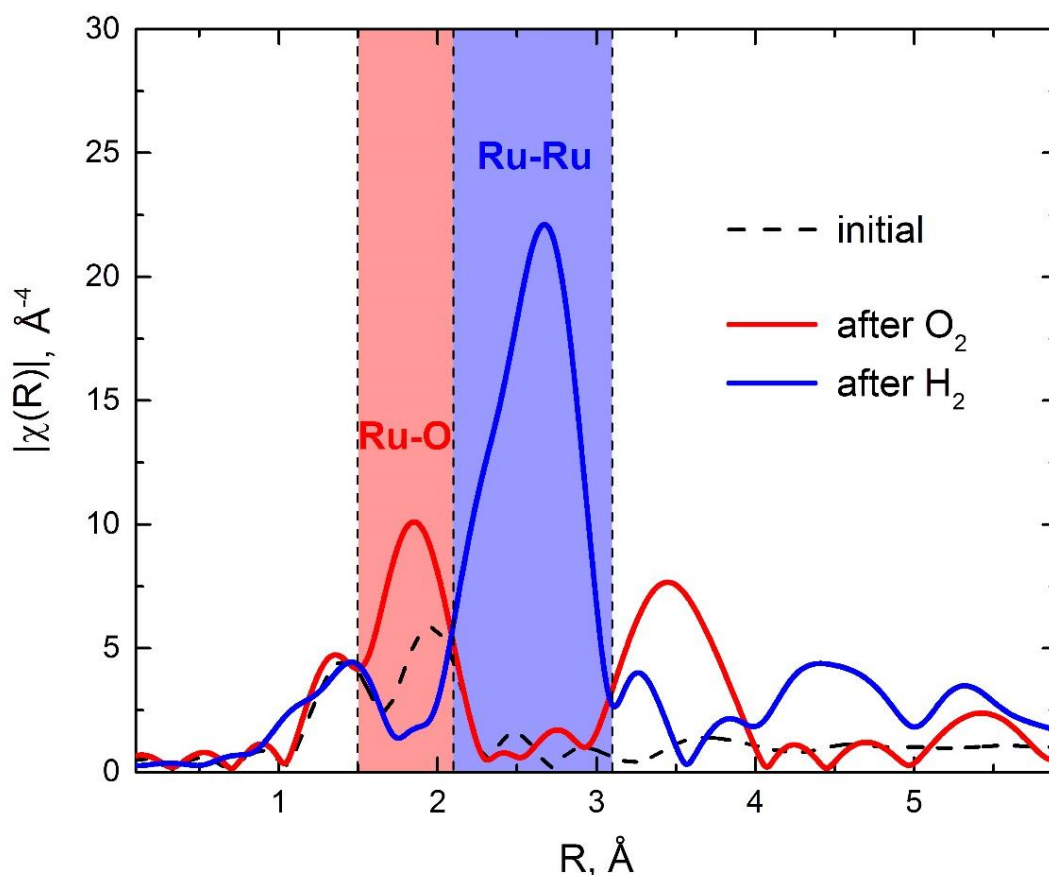


Figure 2.1. EXAFS Fourier-transforms for initial sample (dashed black), after oxidation (red) and after successive reduction (blue).

To estimate the average size of the nanoparticles, the Fourier analysis of EXAFS data was performed. The  $k$ -range from 3 to 12 Å<sup>-1</sup> was taken. The amplitude reduction factor for the Ru foil was determined as  $0.75 \pm 0.05$ . The coordination number for the particles at 180 °C after reduction in H<sub>2</sub> is  $11 \pm 0.8$ , which corresponds to average particle size of  $\sim 10$  nm. These particles must be outside the zeolite pores. At 180 °C there is no evidence of the formation of a metal hydrate phase that we observed in the past at lower temperatures for the bupalladium nanoparticles. This means that in these conditions we have a pure Ru phase.

Figure 2.2top shows the evolution of the Ru K-edge XANES spectra along the oxidation procedure from RT to 450 °C. The differences are small but well detected (see the black dashed spectrum) and allows us to estimate the fraction of the oxide (and the complementary of Ru precursor) along the whole experiment (Figure 2.2bottom).

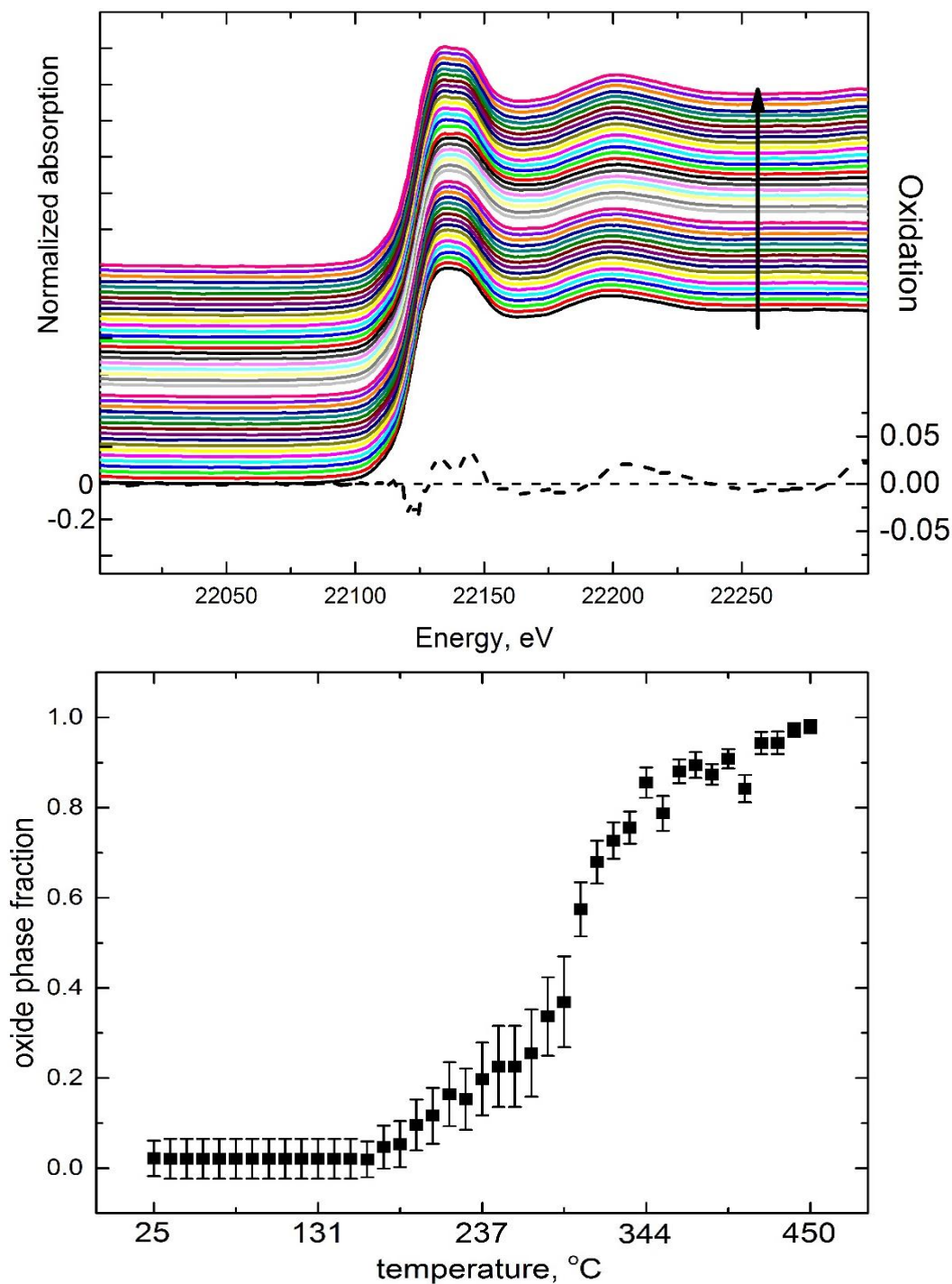


Figure 2.2. Top: evolution of the Ru K-edge XANES spectrum along the formation of ruthenium oxide particles in 20% O<sub>2</sub>/He, ramp from RT to 450 °C. The dashed black spectrum reports the difference spectrum between the first and the long one of the series. Bottom: fraction of the oxide phase estimated from linear combination fit of XANES spectra.

Reduction to Ru metal at 180 °C is complete, see Figure 2.3. Interaction with ammonia modifies the XANES spectrum, indicating the formation of a ruthenium nitrate phase (Figure 2.4). The successive interaction with the alcohol further modifies the XANES spectrum indicating the insertion of carbon atoms at the surface the Ru NPs, either replacing nitrogen and forming a carbide phase or forming a mixed C-N-Ru phases. Again, the changes seem small in the large scale, but when the difference spectrum is plotted (see black dashed curve) they become evident.

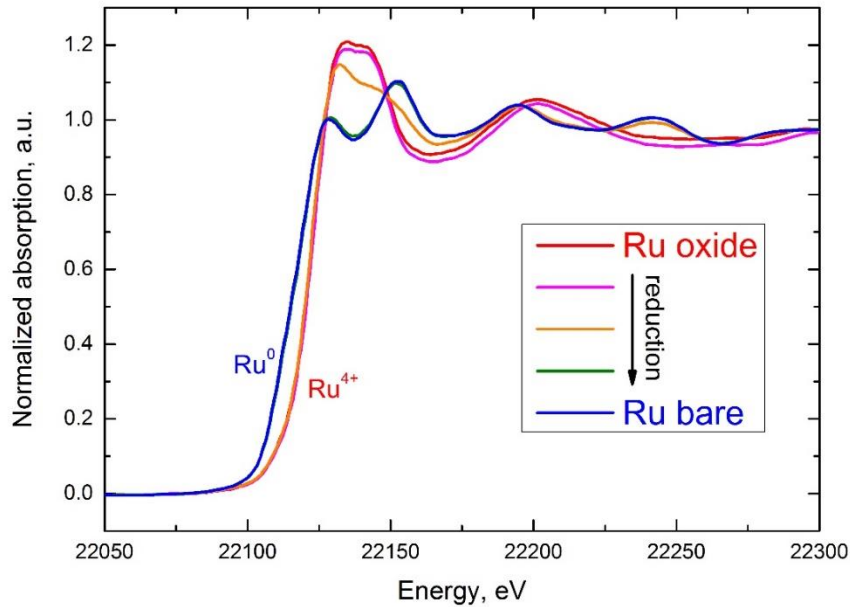


Figure 2.3. Formation of ruthenium nanoparticles, reduction in H<sub>2</sub> at 180 °C as function of time followed by Ru K-edge XANES.

The following pictures (2.4 and 2.5) shows the changes in XANES after exposure of the sample to ammonia (red) and after sending the ammonia through a saturator filled with alcohol (green). It is obvious then the shaping of the near-edge region of the spectra is different. This difference may correspond to Ru-N and Ru-C formation on the surface of the catalyst. The further XANES simulation by FDMNES and FEFF codes are planned to be performed to determine which kind of surface bonds are present.

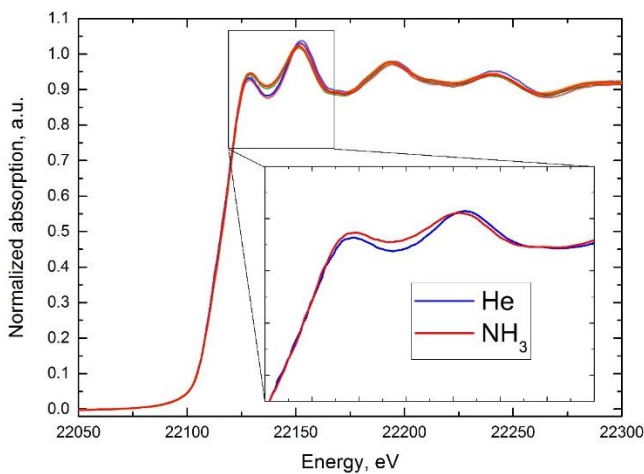


Figure 2.4. Exposure to ammonia at 180 °C, followed by Ru K-edge XANES.

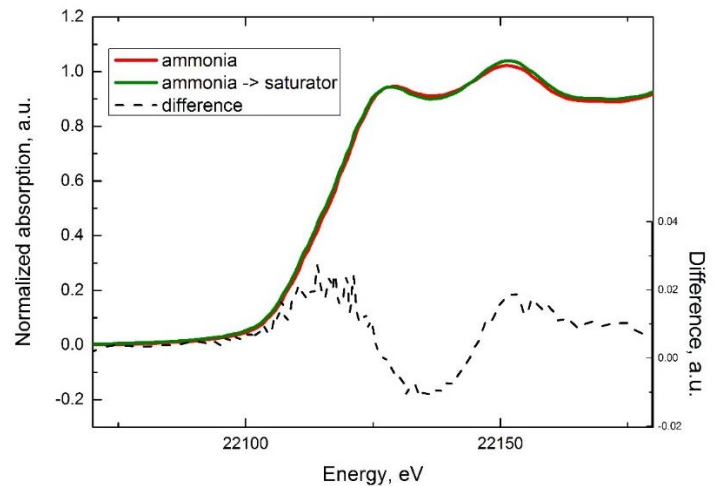


Figure 2.5. Changes observed in the Ru K-edge XANES spectra after sending ammonia through the alcohol saturator at 180 °C.